ARCHIVES OF ELECTRICAL ENGINEERING VOL. 63(2), pp. 149-160 (2014)

DOI 10.2478/aee-2014-0012

Estimators of induction motor electromechanical quantities built on the basis of a machine secondary multi-loop equivalent circuit

A. KAPLON[1], G. UTRATA[2], J. ROLEK[1]

[1] *Chair of Power Electronics, Kielce University of Technology*
Tysiąclecia Państwa Polskiego 17, 25-314 Kielce, Poland
[2] *Institute of Environmental Engineering, Czestochowa University of Technology*
Brzeźnicka 60a, 42-200 Częstochowa, Poland
e-mail: {akaplon/jrolek}@tu.kielce.pl, gutrata@is.pcz.czest.pl

(Received: 18.09.2013, revised:10.01.2014)

Abstract: Contemporary sensorless AC drives require the use of electromechanical quantities estimation. The skin effect occurring in AC machines with solid secondary or with solid secondary elements causes machines of this type to be represented by equivalent circuits containing distributed elements, which makes the analysis of machine electrodynamic states more complicated and hinders the construction of relatively simple and effective estimators of electromechanical quantities. The variability of rotor parameters is modelled, with a good approximation, by the machine secondary multi-loop equivalent circuit with lumped elements. In this paper the construction procedure of electromechanical state variable estimators basing on this type of equivalent circuit will be presented. The simulation investigations of the created electromechanical quantities estimators, performed for the selected states of solid iron rotor AC machine operation will be shown as well.

Key words: electrical machines, induction motor, sensorless control, estimation

1. Introduction

Frequency variability of cage rotor parameters, as a result of the skin effect, causes the deviation of a slip dependent stator impedance characteristic from the circular shape. Motor state variables estimated basing on constant parameters of the induction motor (IM) classical T-type equivalent circuit [1] will not exactly model slip dependent stator or rotor impedance characteristics and thereby properly model a motor electrodynamic state. This problem is even more important in the case of machines with deep-bar cage rotors as well as with rotors manufactured in the form of solid structures where the skin effect is more intensive and therefore the slip dependent stator or rotor impedance characteristics deformation is more noticeable. The deformation of these characteristics has been confirmed through the electromagnetic field analysis carried out by means of the finite element method (Fig. 1).

Algorithmic methods for state variables reconstruction presented in the literature, basing on the mathematical model resulting from the classical structure of the IM equivalent circuit, are sensitive to changes of motor parameters or their incorrect identification. In order to improve the accuracy and reliability of sensorless AC drives, different estimation methods of specified physical quantities have been proposed. The model reference adaptive system (MRAS) concept has been applied for the IM speed estimation [2-6]. In order to improve MRAS speed estimator robustness against motor parameters changes and incorrect identification different modifications of this estimator have been presented i.a. in [7-10]. By using the sliding-mode observers robustness against measurement errors as well as inaccurate identification and changes of system parameters, ensuring estimation errors convergence to zero, can be obtained. An observer sliding surface is determined from the errors between measured and estimated stator currents. As in the case of the MRAS estimator, different modifications of the sliding-mode observer have been also proposed (i.a. [11-15]). Attempts of designing the extended observers and extended Kalman filters with simultaneous estimation of selected motor parameters, can be noticed in the world literature e.g. in [16-21]. The practical application of these types of observers in industrial drive systems is often found to be complicated and requires an advanced microprocessor-based technology. The mathematical model for the motor, on which the above mentioned estimators and observers are created, remains unchanged compared to the classical model.

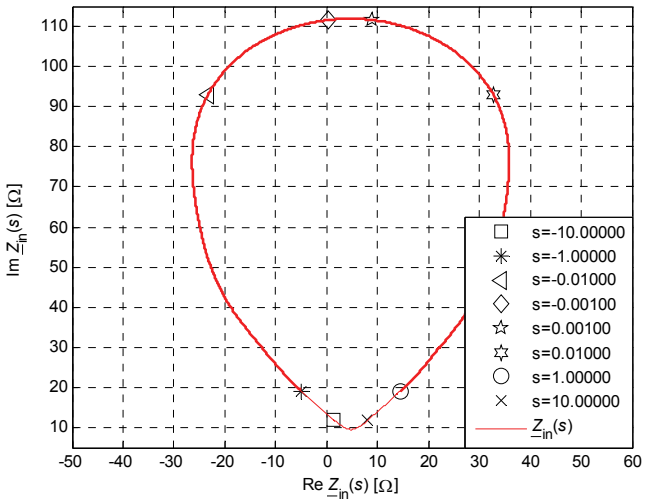

Fig. 1. The slip dependent stator impedance characteristic of the induction motor of Sg 132S-4 type with the solid rotor (steel S235JR)

In the proposed approach estimators of electromagnetic and mechanical state variables are created on the basis of the machine secondary multi-loop equivalent circuit with lumped parameters. Such an equivalent circuit reproduces, with a good approximation, the rotor parameters variability resulting from the skin effect occurring in machine secondary solid parts so that the simultaneous estimation of these parameters is not required.

2. Machine secondary multi-loop equivalent circuit

The frequency domain methods provide the convenient tool for an estimation of equivalent circuit parameters of a symmetrical machine with the skin effect in its secondary. These methods are based on the knowledge of machine impedance frequency characteristics obtained by means of measurement or from electromagnetic field solutions.

The methodology of the spectral inductance $\underline{L}_{1\delta}(\omega)$ determination has been presented in the previous works of the authors [22, 24, 25]. The spectral inductance can be represented by the operational inductance $L_{1\delta}(p)$ (1) resulting directly from the IM equivalent circuit with lumped parameters.

$$L_{1\delta}(p) = L_{\mu} \prod_{i=1}^{n} \left(\frac{1 + pT_i}{1 + p\tau_i} \right), \tag{1}$$

where: $L_{\mu} = L_{1\delta}(p = 0)$, $p = \mathrm{j}\omega$, T_i, τ_i – time constants, p – Heaviside's operator, ω – angular frequency.

The estimation of time constants T_i, τ_i occurring in Equation (1) can be performed by means of the genetic algorithm e.g. in the Matlab-Simulink environment. The estimated time constants of the operational inductance (1) determine R, L parameters of the k-th branch of the machine secondary multi-loop equivalent circuit in accordance with Equations (2) [22].

$$R^{\bullet}_{2(k)} = -L_{\mu} \frac{\prod_{i=1}^{n} (T_k - T_i)\big|_{i \neq k}}{\prod_{i=1}^{n} (T_k - \tau_i)}, \tag{2a}$$

$$L^{\bullet}_{2(k)} = R^{\bullet}_{2(k)} T_k, \tag{2b}$$

where: $R^{\bullet}_{2(k)}$, $L^{\bullet}_{2(k)}$ – lumped parameters of the k-th branch of the machine secondary multi-loop equivalent circuit, referred to the primary side, $k = 1, 2, \ldots, n$, n – number of parallel connected two-terminal consisting of $R^{\bullet}_{2(k)}$, $L^{\bullet}_{2(k)}$ elements.

The frequency characteristics of the spectral inductance and its approximation by the operational inductance are presented in Figure 2.

The result of the operational inductance modal decomposition is the machine equivalent circuit in the form of the parallel connection of the magnetizing inductance L_{μ} and an infinite sequence of two-terminal consisting of $R^{\bullet}_{2(k)}$, $L^{\bullet}_{2(k)}$ elements (Fig. 3).

The IM secondary multi-loop equivalent circuit represents a machine electromagnetic state described by the system of equations in the canonical form (3).

$$\begin{cases} \dfrac{\mathrm{d}}{\mathrm{d}t} \underline{\Psi}_1 = \underline{U}_1 - \mathrm{j}\omega_x \underline{\Psi}_1 - R_1 \underline{I}_1 \\ \dfrac{\mathrm{d}}{\mathrm{d}t} \underline{\Psi}^{\bullet}_{2(k)} = -\mathrm{j}\left(\omega_x - \omega^{\mathrm{r}}\right) \underline{\Psi}^{\bullet}_{2(k)} - R^{\bullet}_{2(k)} \underline{I}^{\bullet}_{2(k)}, \end{cases} \tag{3}$$

where: ω^{r} –rotor electrical angular velocity and $\omega^{\mathrm{r}} = p_{\mathrm{p}}\omega_m$, ω_m – rotor angular velocity, p_{p} – pole pairs, $\underline{\Psi}_1$, $\underline{U}_1$, $\underline{I}_1$, – stator flux, stator voltage and stator current space vectors respectively, $\underline{\Psi}'_{2(k)}$, $\underline{I}'_{2(k)}$ – rotor flux, rotor current space vectors respectively, related to the k-th branch of the machine secondary multi-loop equivalent circuit, referred to the primary side, R_1 – stator phase winding resistance.

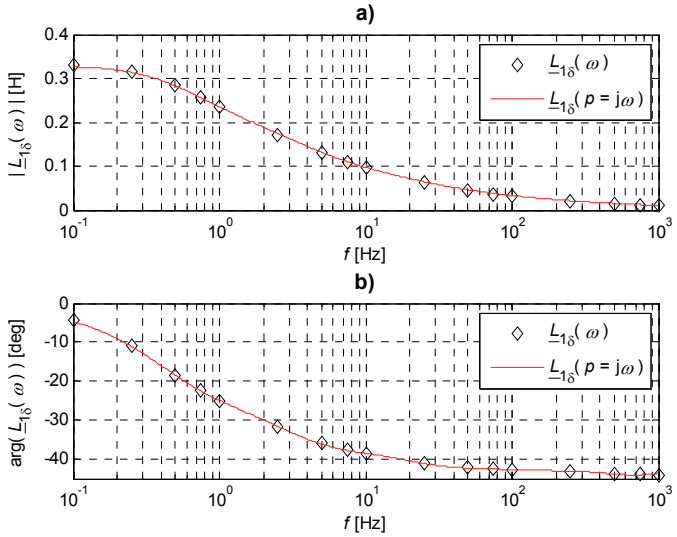

Fig. 2. The frequency characteristics of the spectral inductance $\underline{L}_{1\delta}(\omega)$ and its approximation by the operational inductance $\underline{L}_{1\delta}(p = \mathrm{j}\omega)$: a) module, b) argument

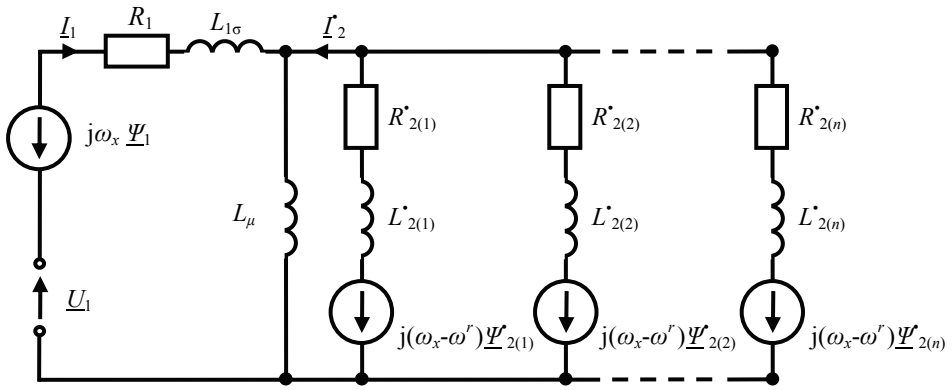

Fig. 3. The machine secondary multi-loop equivalent circuit

The electromagnetic state system of equations in combination with the electromechanical state Equations (4) determine the machine electrodynamic state system of equations, expres-

sed in the reference frame rotating at an arbitrary speed ω_x, thus providing the complete induction machine mathematical model presented in the authors' previous works [22-25].

$$T_e = p_p \operatorname{Re}\left\{ j \underline{\Psi}_1 \underline{I}_1^* \right\}, \tag{4a}$$

$$\frac{d\omega^r}{dt} = \frac{p_p}{J}(T_e - T_{load}), \tag{4b}$$

where: T_e – electromagnetic torque, T_{load} – load torque, J – moment of inertia, superscript * denotes complex conjugate quantity.

3. Methodology of the electromechanical quantities estimation

The machine slip dependent stator impedance characteristic (Fig. 1) and the corresponding secondary multi-loop equivalent circuit (Fig. 3) have been used for the estimation of IM electromechanical quantities.

The structure of the proposed algorithm for the state variables estimation is depicted in Figure 4. Measured instantaneous values of stator voltages and currents are converted to the voltage $\underline{U}_1(t)$ and current $\underline{I}_1(t)$ space vectors respectively, expressed in the reference frame rotating at an arbitrary speed ω_x. The input impedance $\underline{Z}_{in2}(s, t)$, determined by the quotient of the voltage $\underline{U}_1(t)$ and current $\underline{I}_1(t)$ space vectors, is compared with the input impedance $\underline{Z}_{in1}(s)$, resulting directly from the machine equivalent circuit (Fig. 3), in order to determine the slip s and, consequently, the machine angular velocity.

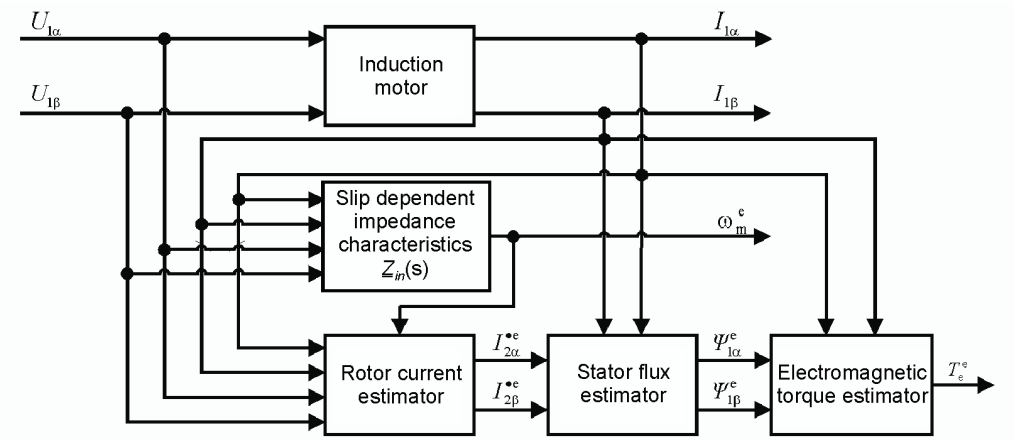

Fig. 4. The algorithm of electromechanical quantities estimation

The determined slip and the mathematical model described by the system of Equations (3) are used to calculate the k-th branch current space vector $\underline{I}^{*e}_{2(k)}(t)$ in accordance with Equation (5). The reconstructed rotor current space vector is utilized for the estimation of the stator flux

space vector and the motor electromagnetic torque in pursuance of Equations (6) and (7) respectively.

$$\underline{I}^{\bullet e}_{2(k)}(t) = \frac{\underline{I}_1(t)(R_1 + \mathrm{j}\omega_1 L_{1\sigma}) - \underline{U}_1(t)}{\frac{R^{\bullet}_{2(k)}}{s^{e}_{avg}(t)} + \mathrm{j}\omega_1 L^{\bullet}_{2(k)}}, \tag{5}$$

where: $L_{1\sigma}$ – inductance associated with the stator leakage flux, including the stator slot, tooth-top and winding overhang leakage flux, ω_1 – stator voltage angular frequency, superscript ^{e} denotes estimated quantities.

$$\underline{\Psi}^{e}_1(t) = (L_{1\sigma} + L_\mu)\underline{I}_1(t) + L_\mu \sum_{i=1}^{n} \underline{I}^{\bullet e}_{2(i)}(t), \tag{6}$$

$$T^{e}_{e}(t) = p_p \,\mathrm{Re}\left\{ \mathrm{j}\underline{\Psi}^{e}_1(t)\underline{I}^{*}_1(t) \right\}. \tag{7}$$

The comparison of the slip dependent stator impedance characteristic resulting directly from the machine secondary multi-loop equivalent circuit $\underline{Z}_{in1}(s)$ with the one determined by the quotient of the voltage and current space vectors $\underline{Z}_{in2}(s,t)$ is presented in Figure 5.

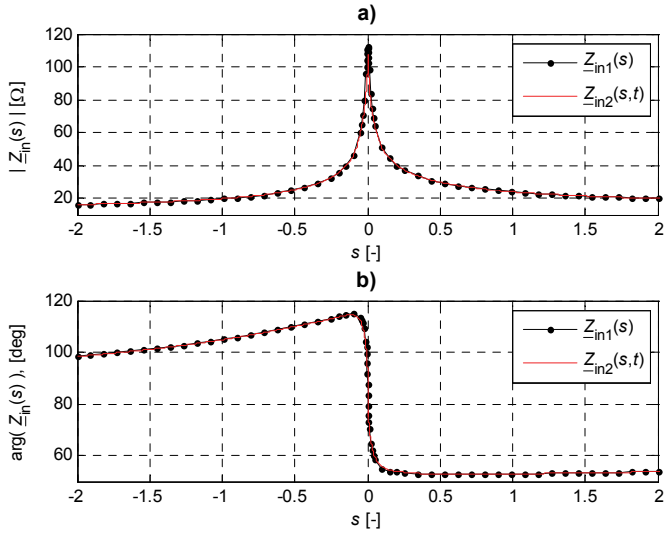

Fig. 5. The slip dependent stator impedance characteristics of the analysed induction motor: a) module, b) argument (description in the text)

The analysis have been conducted for the induction motor of Sg 132S-4 type with the solid rotor manufactured from the magnetic material-steel S235JR. The motor field model has been constructed basing upon the finite element method by using the Elektra Steady-State analysis module of the Opera-3D software. The electromagnetic field distribution on the stator surface in the air gap has been determined. The calculations have been performed at the supply current frequency varied in the range of 0.1÷1000 Hz.

4. Simulation investigations

The simulation experiment leading to the estimation of motor electromechanical quantities is based on the knowledge of the slip dependent stator impedance characteristic and instantaneous values of stator voltages and currents.

In practical applications, instantaneous values of stator voltages and currents are determined by measurement, here for the purpose of simulation investigations the values have been obtained by machine electrodynamic state solutions performed for the selected states of machine operation.

The simulation investigations have been conducted in the Matlab-Simulink environment.

A) Start-up under no load

The waveforms of the motor speed and electromagnetic torque for motor start-up with zero initial speed $n_m(t = 0) = 0$ rpm under the constant load torque of $T_{\text{load}}(t) = 5$ Nm (friction torque) are presented in Figures 6a and 7a (black solid line) respectively. In addition, at the time $t_1 = 4$ s, the step change of the load torque up to the value of $T_{\text{load}}(t_1) = 36$ Nm (Sg 132S-4 nominal torque) occurs. Next, at the time $t_2 = 12$ s, another step change of the load torque to its initial value $T_{\text{load}}(t_2) = 5$ Nm takes place. The system moment of inertia is assumed to be $J = 0.6$ kgm^2.

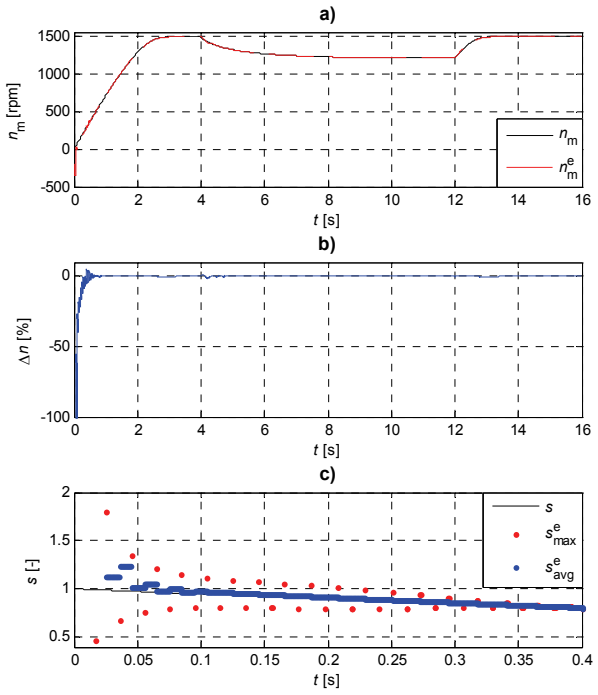

Fig. 6. Waveforms of the motor speed (a), its reconstruction error (b) and the slip (c) for motor start-up under no load (description in the text)

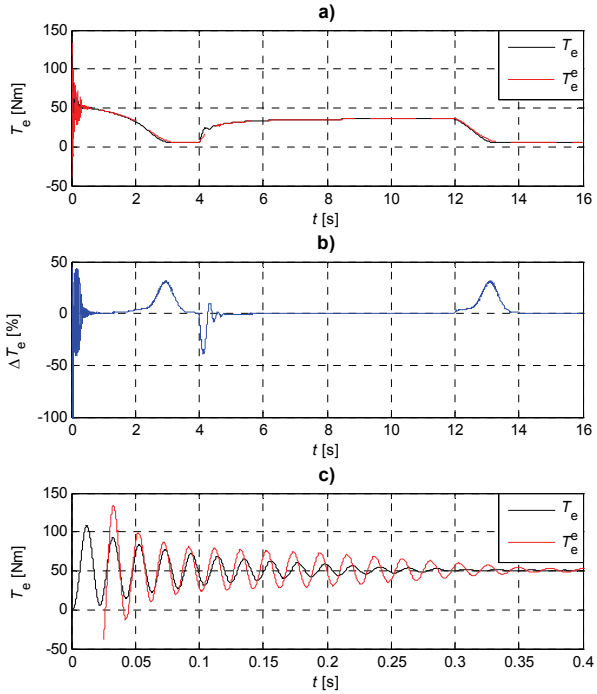

Fig. 7. Waveforms of the motor electromagnetic torque (a), (c) and its reconstruction error (b) for motor start-up under no load (description in the text)

The waveforms of the motor speed and electromagnetic torque estimated on the basis of the stator voltage and current space vectors obtained during motor start-up and load torque changes are presented in the same figures (red dashed line). The waveforms of the motor slip and electromagnetic torque in the initial phase of motor start-up are presented in Figures 6c and 7c respectively.

Additionally, during the motor electromechanical quantities estimation process, the slip error Δs is being observed. The slip error is determined based on the mutual location of the impedance trajectory $\underline{Z}_{we2}(s,t)$ in relation to the impedance trajectory $\underline{Z}_{we1}(s)$. The reconstructed slip values s^e_{max} corresponding to the slip errors close to zero have been presented in Figure 6c (red dot). The averages of these slip values s^e_{avg} are considered as the estimated slip values and used in the further estimation process (blue dotted line in Figure 6c). The action described above allows reducing the oscillations of the estimated slip (speed), especially in the initial phase of machine transients. The proposed algorithm, associated with the reconstructed slip values averaging, introduces the dead time which lasts until the second minimum of the slip error Δs is reached.

B) Start-up under load

The waveforms of the motor speed and electromagnetic torque for motor start-up $n_m(t = 0) = 0$ rpm under the constant load torque of $T_{load}(t) = 36$ Nm are presented in Figures

8a and 9a (black solid line) respectively. The waveforms of the motor slip and electromagnetic torque in the initial phase of motor start-up under load are presented in Figures 8c and 9c respectively. The system moment of inertia is assumed to be $J = 0.6$ kgm^2.

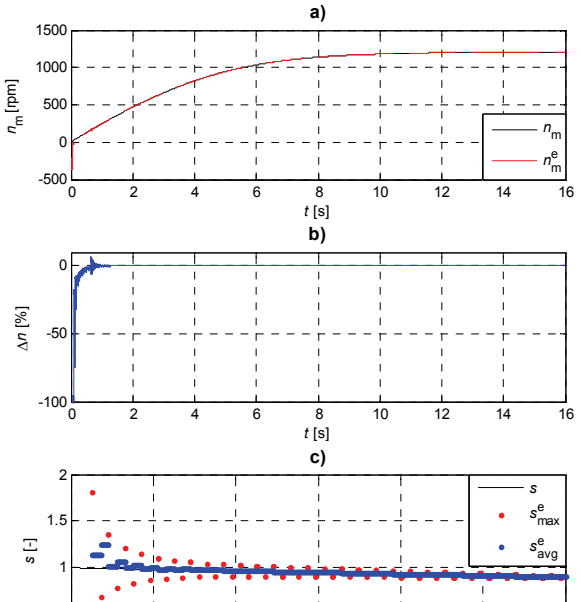

Fig. 8. Waveforms of the motor speed (a), its reconstruction error (b) and the slip (c) for motor start-up under load (description in the text)

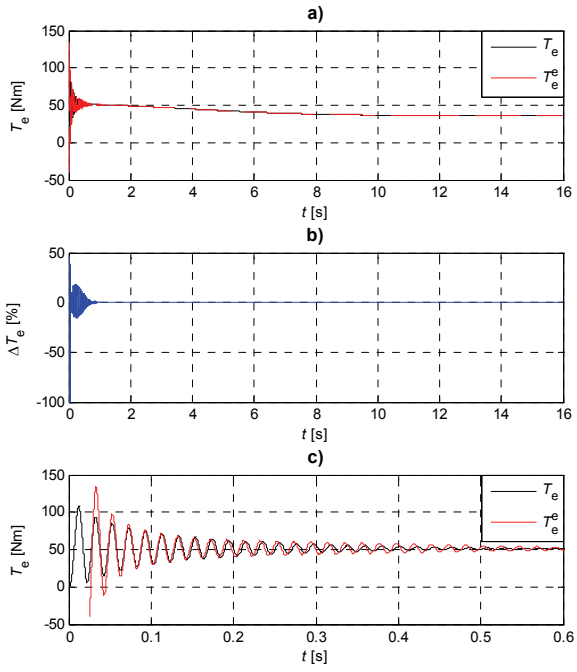

Fig. 9. Waveforms of the motor electromagnetic torque (a), (c) and its reconstruction error (b) for motor start-up under load (description in the text)

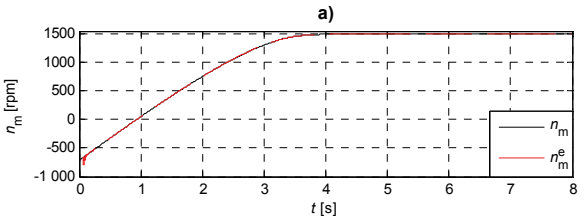

Fig. 10. Waveforms of the motor speed (a), its reconstruction error (b) and the slip (c) for motor reverse operation (description in the text)

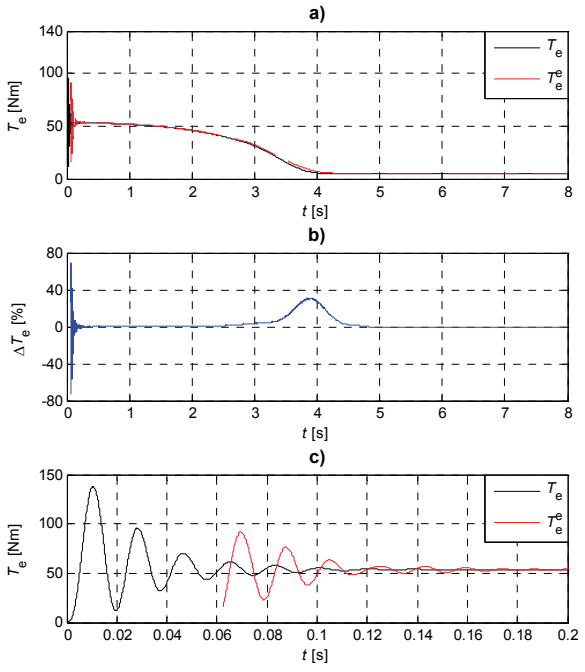

Fig. 11. Waveforms of the motor electromagnetic torque (a), (c) and its reconstruction error (b) for motor reverse operation (description in the text)

C) Reverse operation

The robustness of the proposed algorithm for the electromechanical quantities estimation has been examined under motor reverse operation for the reference speed change from

$n_m(t = 0) = -0.5n_{mn}$ rpm to the no-load motor speed. The load torque and the system moment of inertia are assumed to be $T_{load}(t) = 5$ Nm and $J = 0.6$ kgm^2 respectively. The waveforms of the electromechanical quantities registered during motor reverse operation are presented in Figures 10a and 11a whereas Figures 10c and 11c show the motor slip and electromagnetic torque in the initial phase of the considered case of motor operation.

5. Conclusion

The simulation investigations, carried out for the selected states of machine operation, allow to confirm the usefulness of the presented method for the sensorless estimation of IM electromechanical quantities. The implementation of the proposed method in state variables reconstruction systems requires the measurement of stator voltages and currents instantaneous values, the knowledge of the machine slip dependent stator impedance characteristic and its approximation in the form of the secondary multi-loop equivalent circuit. A slip dependent stator impedance characteristic and equivalent circuit parameters can be determined during the machine tuning process.

References

[1] Paszek W., *Stany nieustalone maszyn elektrycznych prądu przemiennego.* WNT (1986).
[2] Orlowska-Kowalska T., *Sensorless induction motor drives.* Wroclaw University of Technology Press (2003) (in Polish).
[3] Tamai S., Sugimoto H., Yano M., *Speed sensorless vector control of induction motor with model reference adaptive system*, Proceedings of the IEEE – Industry Applications Society Annual Meeting, USA, Atlanta, pp: 189-195 (1987).
[4] Schauder C., *Adaptive speed identification for vector control of induction motors without rotational transducers*, IEEE Transaction on Industry Applications 28(5): 1054-1061 (1992).
[5] Peng F.Z., Fukao T., *Robust speed identification for speed-sensorless vector control of induction motors*, IEEE Transaction on Industry Applications 30(5): 1234-1240 (1994).
[6] Rashed M., Stronach A.F., *A stable back-EMF MRAS-based sensorless low-speed IM drive insensitive to stator resistance variation*, IEE Proceedings – Electric Power Applications,151(6): 685-693, (2004).
[7] Orlowska-Kowalska T., Dybkowski M., *Novel MRAS rotor speed and flux estimator for the sensorless induction motor drive.* Przegląd Elektrotechniczny 82(11): 35-38 (2006) (in Polish).
[8] Orlowska-Kowalska T., Dybkowski M., *Improved MRAS-type speed estimator for the sensorless induction motor drive.* COMPEL 26(4): 1161-1174 (2007).
[9] Niestrój R., Lewicki A., Białoń T., Pasko M., *Reconstruction of magnetic fluxes and rotational speed of induction motor using MRAS-type estimator with Luenberger observer as an adaptive model.* Zeszyty Problemowe-Maszyny Elektryczne 84: 51-57 (2009) (in Polish).
[10] Orlowska-Kowalska T., Dybkowski M., *Stator-current-based MRAS estimator for a wide range speed-sensor less induction-motor driver.* IEEE Transactions on Industrial Electronics 57(4): 1296-1308 (2010).
[11] Rao S., Buss M., Utkin V., *State and parameter estimation in induction motors using sliding modes.* EPE-PEMC 2008. 13th Power Electronics and Motion Control Conference, Poland, Poznan, pp: 2312-2317 (2008).

[12] Lascu C., Boldea I., Blaabjerg F., *A class of speed-sensorless sliding-mode observers for high-performance induction motor drives*, IEEE Transactions on Industrial Electronics 56(9): 3394-3403 (2009).
[13] Hung-Chih Chen, Chun-I Wu, Chia-Wen Chang, Yeong-Hwa Chang, Hung-Wei Lin, *Integral sliding-mode flux observer for sensorless vector-controlled induction motors*, 2010 International Conference on System Science and Engineering (ICSSE), Republic of China (Taiwan), Taipei, pp: 208-303 (2010).
[14] Yeong-Hwa Chang, Chun-I Wu, Hung-Chih Chen, Chia-Wen Chang, Hung-Wei Lin, *Fractional-order integral sliding-mode flux observer for sensorless vector-controlled induction motors*, 2011 American Control Conference (ACC), USA, San Francisco, pp: 190-195 (2011).
[15] Orlowska-Kowalska T., Dybkowski M., Tarchala G., *Performance analysis of the sliding-mode speed observer with magnetizing reactance estimation for the sensorless induction motor driver*, COMPEL 30(3): 968-978 (2011).
[16] Orlowska-Kowalska, T., *Application of the extended Luenberger observer for flux and rotor time constant estimation in induction motor drives*, IEE Proceedings D, Control Theory and Applications 136(6): 324-330 (1989).
[17] Zhang Ch., Nian X., Wang T., Gui W., *Adaptive rotor resistance estimation in the low-speed range of speed sensorless DTC controlled IM drives*, ICIT 2008. IEEE International Conference on Industrial Technology, China, Chengdu, pp: 1-6 (2008).
[18] Hinkkanen M., Harnefors L., Luomi J., *Reduced-order flux observers with stator-resistance adaptation for speed-sensorless induction motor drives.* IEEE Transactions on Power Electronics 25(5): 1173-1183 (2010).
[19] Kang Hyo Park, Cheol Moon, Kee Hyun Nam, Mun Kyu Jung, Young Ahn Kwon, *State observer with parameter estimation for sensorless induction motor.* Proceedings of SICE Annual Conference (SICE), Japan, Tokyo, pp: 2967-2970 (2011).
[20] Bogosyan S., Barut M., Gokasan M., *Sensorless-estimation of induction motors in wide speed range.* COMPEL 26(5): 1288-1303 (2007).
[21] Wang Ch., Li Y., *A novel speed sensorless field-oriented control scheme of IM using extended Kalman filter with load torque observer.* APEC 2008. Twenty-Third Annual IEEE Applied Power Electronics Conference and Exposition, USA, Austin, pp: 1796-1802 (2008).
[22] Kaplon A., *Estimation of the electromagnetic parameters determining the electrodynamic states of the alternating current machines analysed by means of multilayer models*. (Kielce University of Technology Press, 2003) (in Polish).
[23] Kaplon, A., *Estimation of the electrodynamic state of the three-phase induction machine based on its equivalent circuit.* Archives of Electrical Engineering 53(2): 163-177 (2004).
[24] Utrata G., *An influence of magnetic core saturation on equivalent circuit parameters of a linear induction motor.* Proceedings of XII International PhD Workshop OWD 2010, Poland, Wisla, pp: 213-217 (2010).
[25] Utrata G., Kaplon A., *Spectral inductance of the linear motor-space harmonic analysis.* COMPEL 30(3): 1118-1131 (2011).